

4-10-1987

## Rheologic Properties and Kinematics of Emplacement of the Chaos Jumbles Rockfall Avalanche, Lassen Volcanic National Park, California

Dean B. Eppler  
*Arizona State University*

Jonathan H. Fink  
*Portland State University, jon.fink@pdx.edu*

Raymond Fletcher  
*Texas A & M University - College Station*

Let us know how access to this document benefits you.

Follow this and additional works at: [http://pdxscholar.library.pdx.edu/geology\\_fac](http://pdxscholar.library.pdx.edu/geology_fac)



Part of the [Geology Commons](#)

---

### Citation Details

Eppler, D. B., Fink, J., & Fletcher, R. (1987). Rheologic properties and kinematics of emplacement of the Chaos Jumbles rockfall avalanche, Lassen Volcanic National Park, California. *Journal of Geophysical Research: Solid Earth* (1978–2012), 92(B5), 3623–3633.

This Article is brought to you for free and open access. It has been accepted for inclusion in Geology Faculty Publications and Presentations by an authorized administrator of PDXScholar. For more information, please contact [pdxscholar@pdx.edu](mailto:pdxscholar@pdx.edu).



# Rheologic Properties and Kinematics of Emplacement of the Chaos Jumbles Rockfall Avalanche, Lassen Volcanic National Park, California

DEAN B. EPPLER<sup>1</sup>

*Geology Department, Arizona State University, Tempe  
Earth and Space Sciences Division, Los Alamos National Laboratory, Los Alamos, New Mexico*

JONATHAN FINK

*Geology Department, Arizona State University, Tempe*

RAYMOND FLETCHER

*Center for Tectonophysics, Texas A & M University, College Station*

The Chaos Jumbles is a rockfall avalanche deposit that was emplaced by three separate events ~300 years ago. Deposits from each event are distinguishable on the basis of morphology, size variation of large dacitic surface clasts, and by the color of both the matrix and entrained dacitic blocks. Steep lateral and distal deposit margins and surface features such as folds and apparent strike-slip faults indicate that each rockfall avalanche had a finite yield strength and was being actively deformed and sheared throughout the body of the moving deposit, rather than strictly along a basal surface. Kinematic analysis of the three deposits indicates that each had a very low apparent coefficient of friction and was emplaced at velocities of up to ~100 m/s. These data suggest that each rockfall avalanche can be modeled as a pseudoplastic material undergoing flow parallel compression above a frictionless base. This model allows calculation of deposit volumes ranging from ~1.2 to  $1.7 \times 10^8$  m<sup>3</sup> and also suggests that a future rockfall avalanche from the same location would have a more restricted runout than the previous events.

## INTRODUCTION

Rockfall avalanches involve large masses of material ( $>10^6$  m<sup>3</sup>; Hsü [1978]) that move lateral distances up to tens of kilometers at high velocities ( $\sim 10^2$  m/s). Although generally consisting of dry rock debris, they can incorporate significant amounts of snow and ice and can become debris flows by ingestion of water. Rockfall avalanches are among the most destructive mass movement phenomena known. The 1962 and 1970 events at Nevados Huascarán, Peru, for example, killed an estimated total of 30,000 people and destroyed several large towns [Pflaker and Erickson, 1978].

The Chaos Jumbles is a Holocene rockfall avalanche deposit that was emplaced by the collapse of a portion of the Chaos Crags dacite dome complex in Lassen Volcanic National Park. In 1974, the National Park Service closed the \$5,000,000 park campground and visitor facility at Manzanita Lake due to an assessment of the hazards posed by potential continued rockfall avalanche activity from the Chaos Crags [Crandell *et al.*, 1974]. The hazards assessment section of Crandell *et al.* [1974] suggested that in the event of a future rockfall avalanche, there would be insufficient time to evacuate the facilities at Manzanita Lake, some of which were constructed on the previously emplaced deposit.

In order to assess the extent of such future avalanches, we have used the morphology and distribution of the Chaos Jumbles

deposit to construct a model of the behavior of the moving debris and to estimate the kinematics of emplacement of the previous events. The behavior of rockfall avalanche events inferred from these investigations is then used to suggest the behavior and travel distance of a future rockfall avalanche. The results of this study suggest that the rheologic properties of these mass movements during their final stages of emplacement resembled those of a pseudoplastic material with a finite yield strength. We further suggest that a rockfall avalanche originating from the site of the previous events will not travel a sufficient distance to reach Manzanita Lake.

## PREVIOUS WORK

The Chaos Jumbles deposit was first recognized by Williams [1928], who briefly described the deposit margins and surface features and recognized that it had been emplaced farther away from the base of the Chaos Crags than would be expected for typical scree deposits. He attributed the wide extent of the Chaos Jumbles to flow on a muddy basal layer formed from water-saturated Chaos Crags tephra. Although Williams did not address the question of the number of events directly, he implied that the deposit was emplaced by a single rockfall avalanche. Heath [1959, 1960, 1967] studied the Jumbles and, on the basis of conifer succession, tree size variations, and lichenometry, concluded that there was three deposits. The youngest was estimated to be ~270 years old on the basis of tree ring data, and the middle and oldest deposits were estimated to be ~700 and ~1700 years old on the basis of subjective estimates of tree growth and lichenometry. Crandell *et al.* [1974], using essentially the same data, disputed Heath's age differences between events. They found that the oldest trees growing on each of Heath's [1960] "oldest," "middle,"

<sup>1</sup> Now at Science Applications International Corporation, Las Vegas, Nevada.



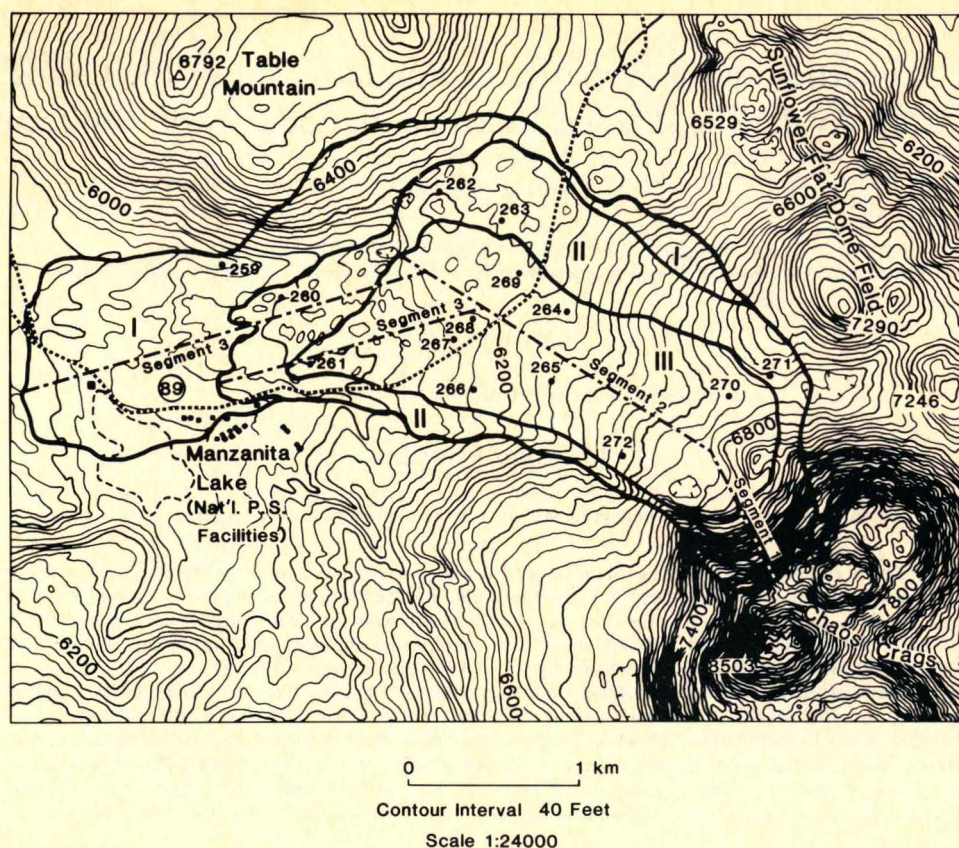


Fig. 1. Distribution of deposits from the three Chaos Jumbles rockfall avalanche events (north is to the top of the page). Segment lines refer to rockfall avalanche path segments used in the kinematic analysis section; note that segment 3 for deposit II is offset  $\sim 400$  m to the south of segment 3 for deposit I. Numbered points are stations used in measurement of the ridge and trough sets.

and "youngest" deposits were between 260 and 290 years old and that there was no evidence that any tree cover was older than 300 years. By implication, it did not appear to Crandell *et al.* [1974] that any deposit was older than 300 years. Both Crandell *et al.* and Heath [1959, 1960, 1967] concurred that deposits from at least three events were recognizable. Radiocarbon age determinations on tree bark from Jeffrey pines drowned when Manzanita Creek was dammed by the stratigraphically oldest deposit give an age of  $290 \pm 50$  years (D. Trimble, personal communication, 1983). On the basis of radiocarbon correction curves of Stuiver [1978], it would appear that the deposit was emplaced between approximately 1540 and 1620 A.D.

#### DEPOSIT DISTRIBUTION, MORPHOLOGY, AND FABRIC

##### Deposit Distribution

The Chaos Jumbles deposit is confined to an L-shaped area formed by the Sunflower Flat dome complex on the east, Table Mountain on the north, and a ridge of glacial moraine on the west (Figure 1). The rockfall avalanche events were strongly channelled by topography, particularly by Table Mountain, where deposit is found up to 100 m above the valley floor. The distal end of the deposit is found  $\sim 4.5$  km away from the base of the Chaos Crags and  $\sim 650$  m below

the top of the breakaway scar. The total area covered by the deposit is  $\sim 6.8$  km<sup>2</sup>.

Three individual deposits were delineated on the basis of conspicuous flow margins or changes in color, angularity, or grain size of large clasts. Each deposit consists of monolithologic breccia of dacite blocks in a matrix of pulverized dacite. Regolith cover is locally developed in areas where the proportion of large surface clasts is low. This regolith accounts for the variations in tree cover originally used by Heath [1959, 1960] to infer different ages for the three deposits.

In general, the lowermost deposit (deposit I) is characterized by surface clasts  $< 0.1$  m with only scarce clasts  $> 1.0$  m. The clasts are predominantly light grey and are subangular to subrounded. Clasts in the middle deposit (deposit II) are also generally  $< 0.1$  m and are light grey and angular to subangular. The uppermost deposit (deposit III) is conspicuously different from the lower deposits and is composed of predominantly coarse-grained, angular pink clasts that have an average grain size larger than deposit I or II. Its surface consists almost entirely of loosely piled, angular clasts that are  $> 0.1$  m and occasionally as large as 5 m. Specific data on clast size variations can be found in the work by Eppler [1984].

The contact between individual avalanche deposits is most pronounced at the distal end of deposit III, where it forms a flow front of coarse blocky debris overlying deposit II (Figure





Fig. 2. Flow front of coarse blocky debris at the distal end of rockfall avalanche deposit III. Fine-grained deposit on the right is rockfall avalanche deposit II. Arrow points to a 30-cm-long scale bar resting on a 1-m-diameter boulder.

2). The distal contact between deposits I and II is more subtle and is characterized by a grain-size decrease that does not coincide with a conspicuous morphology. The lateral margins of all three deposits are less conspicuous than the distal margins and are often characterized by gradual changes in the size of coarse clasts over a <10-m-wide zone, with only a subtle variation in the morphology of the deposit.

#### *Deposit Morphology*

The Chaos Jumbles display morphologic features that are important in determining the motion and rheology of the deposit during emplacement. The features considered here are the margins of each deposit, linear ridge, and trough sets that are oriented transverse to the presumed direction of motion of each rockfall avalanche, and linear grooves that cut deposit III in areas where a change of direction of the rockfall avalanche has taken place.

The margins of the deposit are steep and pronounced and often have a morphology that suggests emplacement as a series of lobate tongues of debris. Parallel to subparallel ridge and trough sets are developed throughout the surface of the deposit and form sets of 2–5 closely spaced ridges with inter-

vening troughs. Although present on all three deposits, they are best seen on the surface of deposit III (Figure 3). In cross section, the individual sets are sinusoidal in shape and appear to be surface folds rather than flow fronts or imbricate thrust sheets. This interpretation is based on the occurrence of linear trains of oxidized boulders that can be traced across several ridge and trough sets without a break or change in orientation. If the ridge-trough sets were imbricate thrusts or flow fronts, these trains would not maintain their integrity unless all of the motion of the deposit was parallel to the direction of the train. Any other direction of motion would cause a break in the train, resulting in several separate segments rather than a single continuous feature.

The amplitudes, orientations, and wavelengths of ridge-trough sets were measured at 14 different locations throughout the Chaos Jumbles, and are shown in Table 1. The wavelength of individual sets varies with location within the deposit. In the proximal section of deposit III, the wavelength is significantly lower than that found in the distal portion. Wavelength and amplitude also vary across the deposit, with the amplitude and wavelength of ridges in the northwestern portion of deposit III being larger than in the southeastern portion. In contrast to deposit III, ridge and trough topography is poorly developed throughout the visible portions of



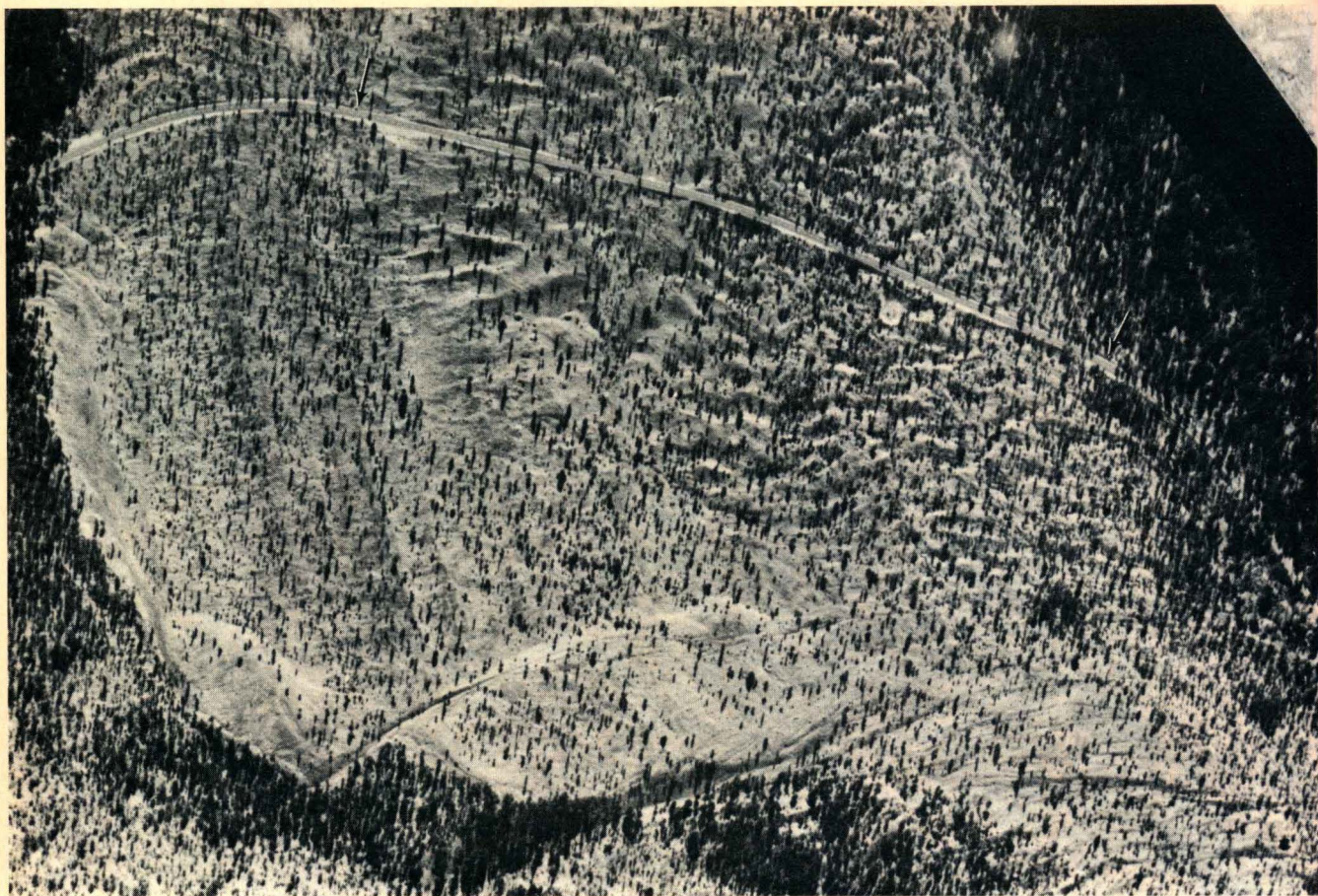


Fig. 3. Ridge and trough topography at the distal end of rockfall avalanche deposit III. Road segment between the arrows is 1 km long.

deposits I and II, and those areas that have ridge-trough sets have less variation in wavelength and amplitude than was seen in deposit III.

South of Table Mountain, where the avalanche path makes a sharp bend, the deposit is cut by a series of narrow elongate grooves that extend for up to 350 m. On aerial photographs, these appear to be strike-slip faults with as much as 200 m of left lateral displacement (Figure 3). The trend of these features is between 50° and 70° to the downstream direction of the rockfall avalanche.

#### *Deposit Fabric*

The horizontal projection of the long axis of surface clasts >0.5 m in size was measured at 15 locations in order to determine any preferred orientations. The results of the measurements are shown in Figure 4.

The rose diagrams at each location indicate that large clasts tend to be oriented in a direction approximately parallel to the topographic gradient of the surface of the deposit and the presumed direction of motion of each rockfall avalanche at that location. This, in turn, suggests that each clast was responding to, and assuming an orientation as a result of the avalanche motion, rather than being carried along in a nondeforming plug of material.

The development of this fabric and the presence of surface features such as streaks, folds, and faults suggests that each rockfall avalanche was behaving like a granular disaggregated

rock mass. These features, in particular, imply that the shear strains related to motion were being transmitted throughout the deposit, rather than being restricted to a basal zone.

#### KINEMATICS OF ROCKFALL AVALANCHE MOTION

Hsü [1975, 1978] reintroduced the concepts developed by Heim [1932] for use in the kinematic analysis of rockfall avalanche events. Central to the work of Heim is the concept that the geometry of the avalanche deposits, and their spatial relation to the source area can be used to estimate the acceleration, velocity, and elapsed time of emplacement of the deposit. Heim developed the concept of the *Farböschung*, which Hsü [1978] defines as the average slope of the course over which the rockfall avalanche deposit moved. The *Farböschung* is determined by measuring the angle formed between the toe of the deposit and the top of the avalanche scar. Heim [1932] proposed that for all landslide-type events, the tangent of the *Farböschung* is a measure of the apparent coefficient of the friction acting on the deposit during emplacement. An important constraint in order to obtain coefficient of friction is that the final velocity  $v_f$  must be equal to zero at the end terminus of the deposit; in the case of the Chaos Jumbles, this is at the end of segment 3. In addition, the relationship of the *Farböschung* to the slope along which the rockfall avalanche moved determines whether it was accelerating or decelerating. If the slope angle is greater than the *Farböschung*, the rockfall avalanche will accelerate, while a slope angle less than



TABLE 1. Ridge and Trough Set Spacing and Orientation

Station	Deposit	Ridge Axis	Wave-length, m	Amplitude, m
259	I	291°	18	1.7
		304°		2.4
		4°	13	1.2
		7°	26	1.9
260	II	356°		2.2
		38°	21	1.3
		72°	32	2.1
		36°	40	2.7
		54°		1.9
261	III	54°	15	3.3
		30°	11	1.5
		35°	23	3.1
		13°	20	1.7
		5°		1.6
262	II	321°	32	2.1
		36°	39	2.7
		54°		1.9
263	II	30°	25	1.6
		40°	22	1.6
		31°	26	2.3
		64°	30	1.0
		68°		2.5
264	III	43°	30	5.5
		47°	45	6.4
		62°		6.4
265	III	46°	35	8.0
		55°	34	6.4
		54°	32	5.1
		34°	21	3.4
		49°		6.4
266	III	88°	40	8.9
		59°	31	3.2
		63°	32	6.4
		28°		8.0
		77°	22	4.6
267	III	89°	27	3.2
		84°		8.0
		53°	37	11.7
268	III	35°	30	6.7
		32°	43	11.2
		37°		8.0
		42°	33	3.2
269	III	34°	45	6.4
		42°	32	5.3
		34°	18	3.2
		41°		5.1
		51°	45	10.2
270	III	69°	49	8.0
		49°	32	6.1
		45°	21	3.9
		34°		4.2
		35°	24	6.8
271	II	31°	47	1.7
		358°	49	7.0
		351°		16.2
		91°	8	1.3
272	III	99°		1.5

Station numbers refer to locations on Figure 1.

the Farböschung will result in deceleration. This information, integrated with the geometry of the deposits can be used to estimate the kinematics of each rockfall avalanche.

The basic equations in Heim's analysis are

$$\tan \alpha = H/L = \mu \quad (1)$$

where  $\alpha$  is the Farböschung,  $H$  is the vertical travel distance,  $L$  is the horizontal travel distance, and  $\mu$  is the apparent coefficient of friction;

$$a = g(\sin \beta - \mu \cos \beta) \quad (2)$$

where  $a$  is the acceleration of the avalanche along a given segment of its path,  $g$  is the acceleration due to gravity, and  $\beta$  is the slope angle along the same path segment;

$$t = v_f - v_i/a \quad (3)$$

where  $t$  is the elapsed time along a given segment of the avalanche path, and  $v_i$  and  $v_f$  are the initial and final velocity along the same path; and

$$v_f = (v_i^2 + 2a(s_f - s_i))^{1/2} \quad (4)$$

where  $s_i$  and  $s_f$  are the position of the beginning and end of the segment in question.

In applying this analysis to the Chaos Jumbles, two assumptions were made: (1) the dome that collapsed was at least as high as the highest point on the breakaway scar, which is ~2500 m mean sea level and (2) the prerockfall avalanche valley floor onto which each rockfall avalanche flowed did not differ sufficiently in slope angle and morphology from the present valley floor to affect the analysis. The first assumption is based on a comparison of the present height of the breakaway scar with the height of the remaining Chaos Crags domes. The second assumption cannot be accurately evaluated, but gives conservative estimates of emplacement parameters, as a steeper slope would give higher accelerations and velocities and shorter emplacement times.

The path over which the avalanche moved can be divided into three segments on the basis of changes in slope angle. The lengths of various segments of the rockfall avalanche path, and calculated values of apparent coefficient of friction, acceleration, velocity, and emplacement time are summarized in Table 2.

Several features of the kinematic analysis are important for our rheologic emplacement model. The first is that the apparent coefficient of friction  $\mu$  is very low. The value of the coefficient of friction for dry granular solids sliding on a smooth surface has been estimated to be 0.6 [Hsü, 1975]. The low values derived imply that if the deposits were emplaced as a sliding rock mass, their basal coefficient of friction was much lower than would be expected. A similar situation has been pointed out by Hsü [1975] for a number of deposits presumably emplaced by similar processes. Hsü has used this feature, in part, to support conclusions that rockfall avalanches are emplaced by a flowing rather than a sliding mechanism. The deposit fabric and surface morphology, which suggest that the shear strain associated with emplacement of the moving deposit was transmitted throughout the body of the deposit, may also support a flowing emplacement process. However, these data are insufficient to unequivocally evaluate this question.

The second feature is that the calculated velocity for each deposit is fairly high, comparable to velocities determined for similar mass movements such as snow avalanches and pyroclastic flows. Similar emplacement velocities have been estimated for historic rockfall avalanches [Hsü, 1978; Pflaker and Erickson, 1978]. Several mechanisms have been suggested to explain these high velocities [e.g., Shreve, 1968; Hsü, 1975; Melosh, 1983], but at present, the debate remains unresolved.

#### RHEOLOGIC MODELING OF THE ROCKFALL AVALANCHE EVENTS

Several types of morphologic and structural evidence can be used to constrain a model for the rheologic behavior of the



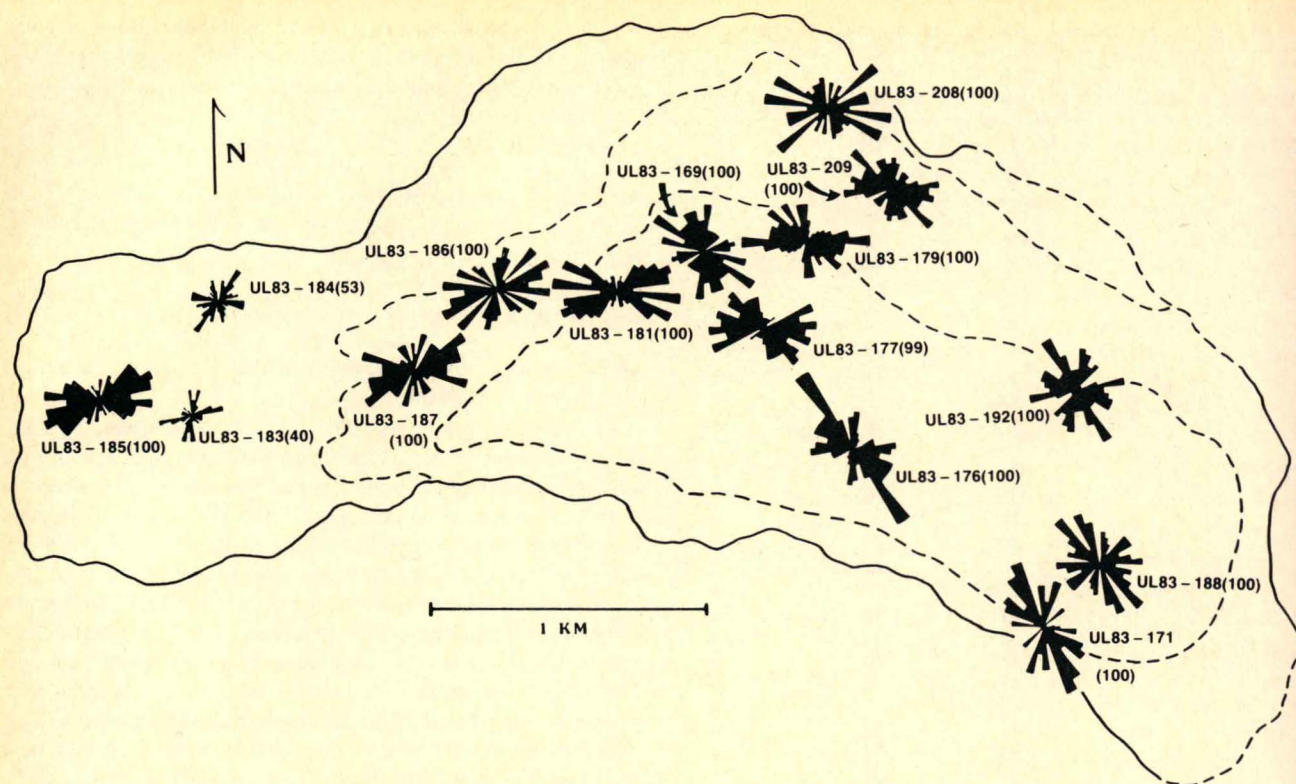


Fig. 4. Rose diagrams prepared using the azimuth of surface clasts  $>0.5$  m in diameter. Numbers in parentheses to the right of the station number indicate the size of the sample for each rose diagram.

Chaos Jumbles rockfall avalanches during emplacement. This evidence can be used to infer the rheologic state of these deposits only during their terminal stages of movement; it is not clear whether this rheologic model accurately describes the deposits during the whole sequence of emplacement. However, the model we will describe below appears to allow reasonable predictions of parameters that can be independently estimated, such as deposit volume, and we feel that it is useful as a first-order approximation of the behavior of the moving debris.

The significant heights of lateral margins of the deposit indicate that the moving debris had a finite yield strength [Johnson, 1970]. We can estimate this strength by assuming that each avalanche spread and thinned laterally until the basal stress was equal to the yield strength of the deposit. The basal shear stress  $\tau_b$  is

$$\tau_b = \rho g H \sin \theta \quad (5)$$

where  $\rho$  is debris density,  $H$  is marginal thickness, and  $\theta$  is the

TABLE 2. Emplacement Parameters Calculated for the Chaos Jumbles Rockfall Avalanche Events Using the Method of Heim [1932]

	$H$ , m	$L$ , m	$\alpha$	$\beta$	$\mu$	$s_i$ , m	$s_f$ , m	$a$ , $\text{m s}^{-2}$	$v_i$ , m/s	$v_f$ , m/s	$t$ , s
Rockfall Avalanche 1	770	5040	8.7°		0.15						
Segment 1				45°		0	530	5.9	0	79	14
Segment 2				6°		530	2570	-0.4	79	68	28
Segment 3				2°		2570	5040	-1.1	68	0	62
Rockfall Avalanche 2	651	3480	10.6°		0.19						
Segment 1				45°		0	530	5.6	0	55	10
Segment 2				6°		530	2090	-0.8	55	23	40
Segment 3				2°		2090	3660	-1.5	23	0	15
Rockfall Avalanche 3	430	2040	11.9°		0.21						
Segment 1				45°		0	860	5.5	0	97	18
Segment 2				6°		860	3010	-1.0	97	0	97

$H$ , vertical fall distance from breakaway scar to distal deposit edge;  $L$ , horizontal travel distance;  $\alpha$ , angle up from horizontal of a line connecting the distal edge of the deposit with the top of the breakaway scar;  $\beta$ , slope angle of the segments along which each rockfall avalanche moved;  $\mu$ , apparent coefficient of friction;  $s_i$ , position of initial point for a given segment;  $s_f$ , position of final point for a given segment;  $a$ , acceleration;  $v_i$ , initial velocity;  $v_f$ , final velocity; and  $t$ , time calculated for the rockfall avalanche to cross a given segment.



slope angle of the terrain underlying the deposit [Moore et al., 1978]. For margin heights of 3–5 m and an assumed density of 2000 kg/m<sup>3</sup>, we can calculate a yield strength at the deposit margin of 0.6 to 1.0 × 10<sup>4</sup> Pa, comparable to andesite lava flows [Moore et al., 1975].

The presence of subparallel strike-slip faults where the avalanche was compressed (Figure 3) indicates that it was capable of shearing along discrete slip surfaces. This type of deformation is typical of plastic materials that have finite yield strengths [Johnson, 1970]. Such plastic behavior has been proposed for phenomena ranging in scale from the collision of continental plates [e.g., Tapponier and Molnar, 1976] to deformation of single crystals [e.g., Weertman, 1970] and is consistent with the large strength indicated by the heights of the deposit margins.

Transverse ridges are found on the surface of much of the deposit, but are concentrated at sites of probable compression. Similar ridges have been described on the Elm, Blackhawk, and Frank landslide deposits [Shreve, 1968]. The regular spacing of these ridges suggests that they formed in response to a surface folding instability as a result of flow parallel compression. Many materials, when subjected to this type of compression, develop periodic surface structures whose wavelengths depend on the rheology and geometry of the deforming medium. The folding process involves selective amplification of certain components within the wavelength spectrum of the initially irregular upper surface. The wavelength  $L$  that grows most rapidly tends to dominate the final surface configuration, appearing as the most common ridge spacing (Figure 5).

In order for a folding model to be applicable, the ridge and trough wavelengths should be concentrated about a single value. Measurements made on deposit III appear to show a preferential development of wavelengths in the range of 31–35 m (Figure 6). Deposit II shows a slight concentration in the 21- to 25-m wavelength range, whereas deposit I does not show any apparent preferred wavelength. It is not clear whether deposits I and II are undersampled or did not undergo surface folding. Regardless, we feel that the measurements for

deposit III show sufficient wavelength selection to justify further analysis.

To produce a regular surface fold wavelength by compression, the debris rheology must satisfy certain criteria. There are a few possible models for deformation of debris flows that are both geologically plausible and sufficiently simple to be mathematically tractable. A broad range in rheological behavior can be encompassed by assuming that the debris behaved like a uniform, incompressible, and isotropic power law fluid. The strain rate components  $\varepsilon_{ij}$  are related to the components of the deviatoric stress  $S_{ij} = \sigma_{ij} - 1/3\sigma_{kk}\delta_{ij}$  by

$$\varepsilon_{ij} = BJ_2^{(n-1)/2} S_{ij} = (\frac{1}{2}\eta)S_{ij} \quad (6)$$

where  $J_2 = 1/2 S_{ij}S_{ij}$ ,  $n$  is the power law exponent,  $B$  is a constant, and  $\eta$  is a stress-dependent effective viscosity. An additional simplifying assumption is that the debris shortened above a frictionless surface. This is justified by the results of the kinematic analysis presented earlier (Table 2), which indicates that apparent coefficient of friction was very low.

More complicated models might consider friction at the base or a depth dependence of either  $n$  or  $\eta$ . The only model considering these factors that has been previously treated is the case of shortening of Newtonian fluid whose viscosity decreases exponentially with depth [Fink and Fletcher, 1978]. We are assuming that the degree of accuracy of the observations presented here does not justify applying more complicated models.

In the analysis, we have therefore considered a layer of power law material of thickness  $h$  undergoing uniform shortening at a rate  $\bar{\varepsilon}$  above a frictionless sliding surface. If we introduce a cylindrical perturbation, the upper surface may be represented as

$$z = h + A \cos(lx) \quad (7)$$

where  $l = 2\pi/L$  is the wave number. The goal of the perturbation analysis is to determine the wavelength  $L$  that maximizes the growth rate. Following a procedure similar to that outlined in the works by Fletcher (1974) and Fink and Fletcher [1978] we find

$$\begin{aligned} (1/A)(dA/dt) = q\bar{\varepsilon} \\ = -\bar{\varepsilon} + 2n\bar{\varepsilon}[2 \sin \beta k + (n-1)^{1/2}(e^{\alpha k} - e^{-\alpha k})] \\ \cdot [2 \operatorname{sgn}(\varepsilon) \sin \beta k - (1-1/n)^{1/2} \\ \cdot (e^{\alpha k} + e^{-\alpha k} - 2 \cos \beta k)/S^*k] \end{aligned} \quad (8)$$

where  $\alpha = (1/n)^{1/2}$ ,  $\beta = (1-1/n)^{1/2}$ ,  $k = 2lh = 4\pi h/L$ , and  $S^* = 2\eta\bar{\varepsilon}/\rho gh = \tau/\rho gh$  is the ratio of the shear stress associated with the mean shortening  $\tau$  to the lithostatic stress at the base of the layer.

In order for a well-defined wavelength to be selected during a moderate amount of shortening,  $q$  must be sufficiently large; 10 is commonly taken as a minimum value. Figure 7a shows  $q$  versus dimensionless wave number  $k$  for various values of the power law exponent  $n$ . These results, which are for the limiting case in which gravity is not important ( $S^* \rightarrow \infty$ ), indicate that the wave number of the component that grows most rapidly  $k_d$  decreases only slightly as  $n$  goes from  $\Pi$  to 100. Figure 7a also shows that values of  $q$  will be greater than 10 only for large

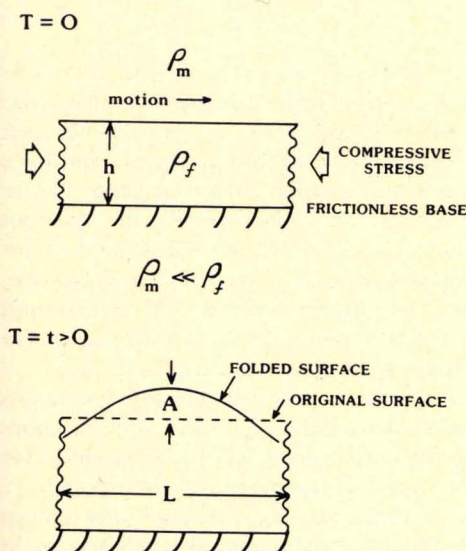


Fig. 5. Rheologic model used to interpret the ridge and trough sets and to determine the average thickness of each rockfall avalanche deposit.



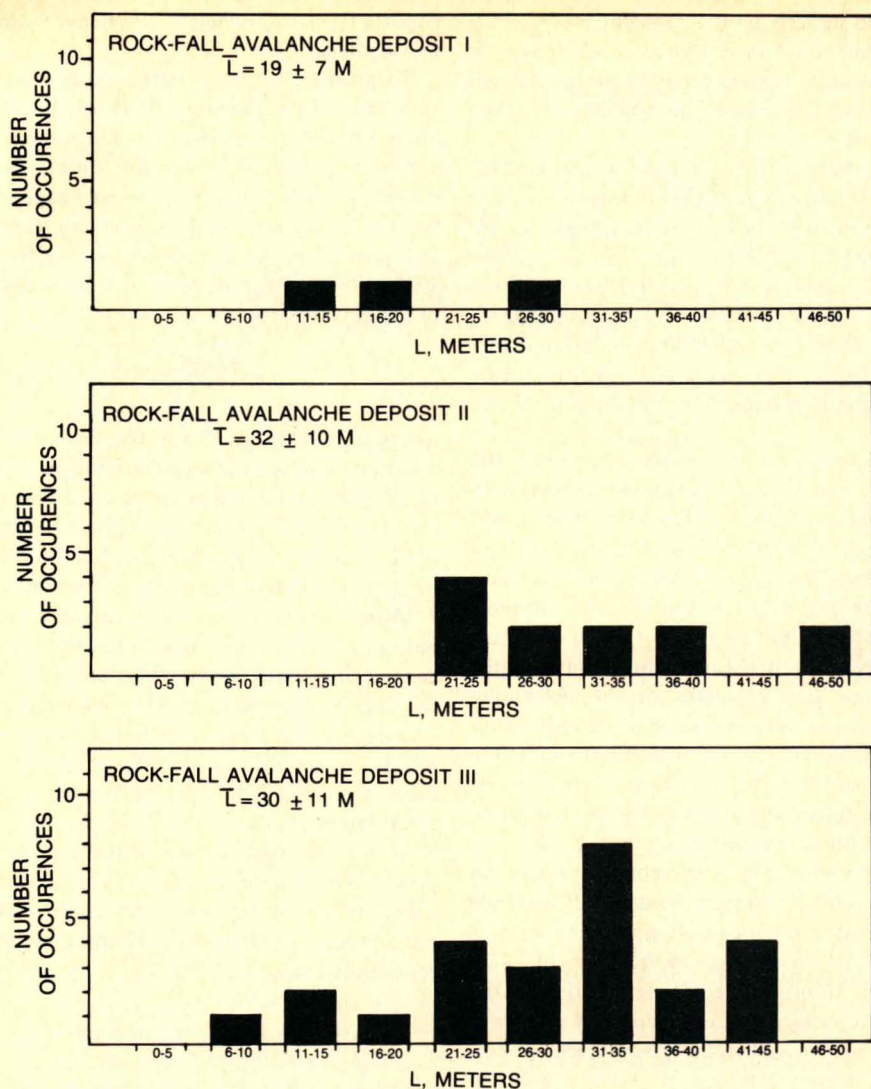


Fig. 6. Frequency distribution of measured wavelengths on the three rockfall avalanche deposits. Selection of a dominant wavelength appears to be developed best in ridge and trough sets formed on rockfall avalanche deposit III.

values of  $n$ , which indicates that surface folding on a debris flow will only occur if the active debris has a strongly pseudo-plastic rheology ( $n \gg 1$ ).

Figure 7b shows the results when the debris has a finite yield strength  $\tau$  that is allowed to vary, while the power law exponent  $n$  is assumed to stay constant and very large. Here  $q/n$  versus  $k$  is shown for different values of  $S^* = \tau/\rho gh$ . Again,  $k_d$  varies only from 4.5 to  $2\pi$  ( $L_d/h = 2.8$  to 2) as  $S^*$  goes from infinity to zero. For any large value of  $n$ , large  $q$  and hence folding is favored by a large value of the debris strength  $\tau$ .

We can conclude from these results that regularly spaced folds observed on the surface of a debris flow imply that the active Chaos Jumbles rockfall avalanche had a relatively high strength and a high power law exponent and that the ridge spacing ranged between 2.0 and 2.8 times the flow thickness. If these results are applied to the ridge spacing data from the Chaos Jumbles, we can estimate the thickness of the deposit.

Table 3 presents the calculated values of deposit thickness for ridge and trough measurement stations throughout each of

the three Chaos Jumbles rockfall avalanches. These values are based on the average measured ridge spacing at each station. Table 4 gives the calculated average deposit thickness, assuming a uniform distribution of deposit, and the calculated total deposit volume based upon thickness. If it is assumed that the deposit had a high strength, the corresponding deposit volume is  $\sim 1.7 \times 10^8$  m<sup>3</sup>. Assumption of low strength for the deposit gives a calculated deposit volume of  $\sim 1.2 \times 10^8$  m<sup>3</sup>. These figures agree favorably with deposit volumes estimated by Williams [1932], Crandell *et al.* [1974], and MacDonald (unpublished manuscript).

These estimates can be compared with a calculation of the volume of the dome that collapsed to form the Chaos Jumbles deposit. If the missing dome had a total height and morphology similar to the remaining domes, the calculated volume of the deposit would be  $\sim 1.1 \times 10^8$  m<sup>3</sup>. The discrepancy between the calculated and estimated values may be the result of increased void space in the deposit relative to the original dome or to inaccuracies in estimating the height and width of



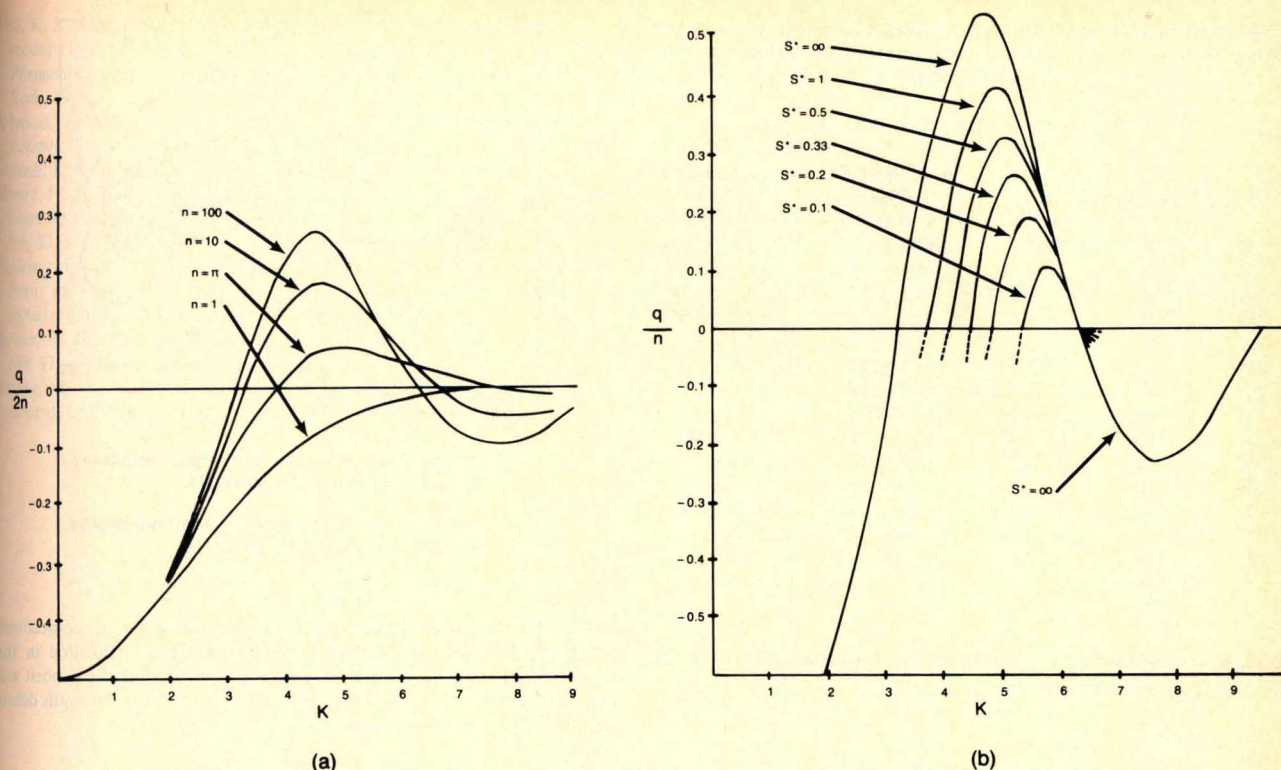


Fig. 7. (a) Plot showing the dimensionless amplification factor ( $q/2n$ ) versus wave number ( $k = 4\pi h/L$ ;  $h$ , layer depth,  $L$ , wavelength) for four values of power law exponent  $n$  for the case of high-strength material. Folding instability requires  $q > 0$  and strong wavelength selection requires  $q > 10$ . Plot indicates that as  $n$  approaches infinity, the system becomes increasingly unstable. Results for the low-strength case are similar, with the maximum amplification shifting to larger  $k$ , resulting in shorter wavelengths. (b) Plot of amplification factor ( $q/n$ ) versus dimensionless wave number  $k$  for various values of strength parameter  $S^* = \tau/\rho gh$  ( $n$  is assumed to be large ( $> 30$ ), based upon Figure 7a),  $k$  ranges from  $2\pi$  to 4.5 as  $S^*$  increases, but  $q$  is only large enough to promote folding for  $S^* > 1$ . Negative values of  $q/n$  are shown only for the case of  $S^* = \infty$ .

the original dome. This estimate is sufficiently close to the calculated volume to suggest that the thickness estimates derived from the folding analysis are reasonable.

In summary, the presence of marginal scarps, strike-slip faults, and regularly spaced surface ridges suggest that the Chaos Jumbles deposits were emplaced as high yield strength materials. This suggestion, along with the kinematic analysis, indicates that the moving rockfall avalanche can be modeled as a pseudoplastic material that was moving over a nearly frictionless base. The position and spacing of surface ridges further indicate that the deposits were undergoing flow parallel compression during the final stages of movement.

#### HAZARDS POSED BY FUTURE COLLAPSE OF THE CHAOS CRAGS

This examination of the Chaos Jumbles deposit permits us to evaluate the potential hazard associated with a future rockfall avalanche originating from the same breakaway scar as the previous three. This evaluation is based on trends seen in the kinematic analysis; in particular, that with successive rockfall avalanches the apparent coefficient of friction becomes greater, and the distance each rockfall avalanche traveled and the width of the resulting deposit is less. We further assume that such an event might occur without sufficient warning to evacuate National Park Service facilities at Manzanita Lake. We do not consider an event such as renewed volcanic activity at the Chaos Crags that would most likely

have precursor events which could be geophysically monitored and would allow sufficient time to evacuate potential danger areas.

The assumptions made in this evaluation are as follows: (1) a fourth rockfall avalanche will have no more than 10% of the aggregate volume of all three rockfall avalanche deposits, based on an estimate of the amount remaining of the Chaos Crags dome that did not collapse in the first three events; (2) the deposit will have a strength-dependent thickness that ranges from a minimum of 10 m to a maximum of 20 m; (3) the apparent coefficient of friction of the avalanche will be between 0.15 and 0.21; (4) the width of the resulting deposit will be no greater than deposit III; (5) this avalanche will originate at the same breakaway scar as the previous three and involve the material from the original dome that remains in the breakaway scar; and (6) the driving force for the new rockfall avalanche will be gravity, with no component of kinetic energy added by lateral explosive events.

By assuming that the volume will be distributed at a uniform thickness across a constant width, it is possible to solve for the travel distance for the two cases of high- and low-strength material. For the high-strength case, the travel distance is  $\sim 1700$  m; for the low-strength case, the travel distance is  $\sim 2000$  m. The resulting distributions are shown in Figure 8. This prediction suggests that in either case, the fourth event will not travel as far as Manzanita Lake, al-



TABLE 3. Thickness of Rockfall Avalanche Deposit at Ridge and Trough Measurement Locations, Based on Average Wavelength  $L$  at Each Location

Station	Deposit	$\bar{L}$ , m	$h$ , m	
			High-Strength Case	Low-Strength Case
259	I	$19 \pm 7$	$9.5 \pm 3.5$	$6.8 \pm 2.5$
260	II	$31 \pm 10$	$15.5 \pm 5.0$	$11.1 \pm 3.6$
261	III	$17 \pm 5$	$8.5 \pm 2.5$	$6.1 \pm 1.8$
262	II	$36 \pm 5$	$18.0 \pm 2.5$	$12.9 \pm 1.8$
263	II	$26 \pm 3$	$13.0 \pm 1.5$	$9.3 \pm 1.1$
264	III	$38 \pm 11$	$19.0 \pm 5.5$	$13.6 \pm 3.9$
265	III	$31 \pm 7$	$15.5 \pm 3.5$	$11.1 \pm 2.5$
266	III	$34 \pm 5$	$17.0 \pm 2.5$	$12.1 \pm 1.8$
267	III	$25 \pm 4$	$12.5 \pm 2.0$	$8.9 \pm 1.4$
268	III	$37 \pm 7$	$18.5 \pm 3.5$	$13.0 \pm 2.2$
269	III	$32 \pm 11$	$16.0 \pm 5.5$	$11.4 \pm 3.9$
270	III	$37 \pm 13$	$18.5 \pm 6.5$	$13.2 \pm 4.6$
271	II	$40 \pm 14$	$20.0 \pm 5.0$	$14.3 \pm 5.0$
272	III	8	4.0	2.9

though an avalanche with unusually low strength could be deposited on a portion of the park road.

### CONCLUSIONS

The Chaos Jumbles appears to have been emplaced by three separate rockfall avalanche events that occurred  $\sim 300$  years ago during the collapse of the northernmost Chaos Crags dacite dome. Surface features, such as sinusoidal folds, grooves that appear to be strike-slip faults, and steep lateral and distal margins all suggest that the debris forming the deposits was emplaced as a high yield strength material that was capable of deforming and shearing, rather than as a plug of nondeforming material being carried along on a deforming basal layer. A kinematic analysis, as first derived by Heim [1932], indicates that the apparent coefficient of friction on the base of each avalanche was 3 to 4 times less than would be expected for a sliding body of dry granular materials. These data allow each event to be modeled as the deformation of a pseudoplastic material that was undergoing flow parallel compression in the later stages of emplacement. Use of this model allows an estimation of the volume of the deposit which is similar to estimates made by inferring the size of the collapsed dome. An estimation of the distribution of deposits from a fourth rockfall avalanche, based upon this rheologic model and the results of the kinematic analysis, suggest that such an event would not travel as far as Manzanita Lake.

TABLE 4. Calculated Average Deposit Thickness and Volume for Each Rockfall Avalanche

	Average Deposit Thickness, m		Average Deposit Volume, m <sup>3</sup>	
	Low Strength	High Strength	Low Strength	High Strength
Deposit I	6.8	9.5	$4.4 \times 10^7$	$6.1 \times 10^7$
Deposit II	11.4	16.0	$5.0 \times 10^7$	$7.0 \times 10^7$
Deposit III	10.7	15.0	$2.6 \times 10^7$	$3.6 \times 10^7$
Total deposit volume			$1.2 \times 10^8$	$1.7 \times 10^8$

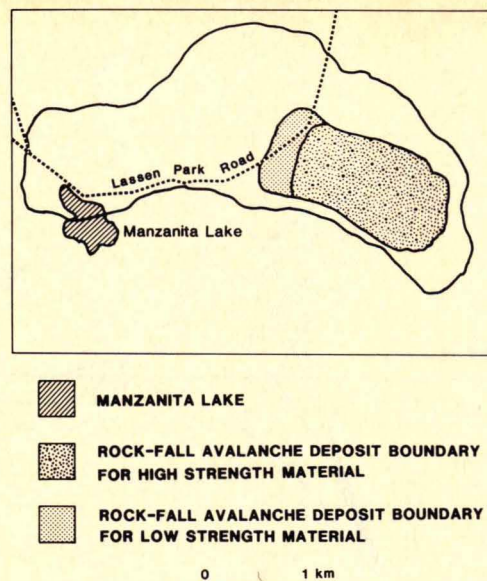


Fig. 8. Suggested distribution of deposit from a conjectured fourth rockfall avalanche, based on assumptions delineated in the text. Note that (1) for neither case does it appear that the deposit will reach Manzanita Lake and (2) only in the case of low-strength debris will the deposit cover a portion of the park road.

**Acknowledgments.** The authors acknowledge the assistance of the National Park Service personnel at Lassen Volcanic National Park. In particular, Lauren Compton, Kathy Mauler, Gail Nash, and Ellis Richard assisted in making many of the field measurements used in this study. In addition, Susan Selkirk of Arizona State University Geology Department and Florence Fujita of Los Alamos National Laboratory drafted many of the illustrations, Dan Ball of Arizona State University provided photographic assistance, Marcia Jones of Los Alamos National Laboratory helped with the typing of the manuscript, and Debbie Trimble of the U.S. Geological Survey at Menlo Park gave permission to use her radiocarbon age determinations for trees killed by the Chaos Jumbles. This paper benefitted from discussions with Richard Vance and Ellis Richard of the National Park Service, Bob Christiansen and Donna Marron of the U.S. Geological Survey, and Mike Malin of Arizona State University, and from critical reviews by H. J. Melosh and D. R. Crandell. Funding of this study came primarily from National Science Foundation Environmental Geosciences grant EAR8313091 and a grant from the Associated Students of Arizona State University. J. F.'s participation was supported by National Aeronautics and Space Administration grant NAGW 529 to Arizona State University and by National Science Foundation grant EAR8309500.

### REFERENCES

- Crandell, D. R., D. R. Mullineaux, R. S. Sigafos, and M. Rubin, Chaos Crags eruptions and rock-fall avalanches, Lassen Volcanic National Park, California, *J. Res. U.S. Geol. Surv.*, 2, 49–61, 1974.
- Eppler, D. B., Characteristics of volcanic blasts, mudflows and rock-fall avalanches in Lassen Volcanic National Park, Ph.D. dissertation, Ariz. State Univ., Tempe, 1984.
- Fink, R. H., and R. C. Fletcher, Ropy pahoehoe: Surface folding of a viscous fluid, *J. Volcanol. Geotherm. Res.*, 4, 151–170, 1978.
- Fletcher, R. C., Wavelength selection in folding of a single layer with power-law rheology, *Am. J. Sci.*, 274, 1029–1043, 1974.
- Heath, J. P., Dating Chaos Jumbles, an avalanche deposit in Lassen Volcanic National Park, *Am. J. Sci.*, 257, 537–538, 1959.
- Heath, J. P., Repeated avalanches at Chaos Jumbles, Lassen Volcanic National Park, California, *Am. J. Sci.*, 258, 744–751, 1960.
- Heath, J. P., Primary conifer succession, Lassen Volcanic National Park, *Ecology*, 48, 270–275, 1967.
- Heim, A., *Bergsturz und Menschenleben*, 218 pp., Fretz and Wasmuth, Zurich, 1932.
- Hsü, K. J., Catastrophic debris streams generated by rockfalls, *Geol. Soc. Am. Bull.*, 86, 129–140, 1975.



- Hsü, K. J., Albert Heim: Observations on landslides and relevance to modern interpretations, in *Rockslides and Avalanches*, vol. 1, *Natural Phenomena*, edited by B. Voight, pp. 71–93, Elsevier Science, New York, 1978.
- Johnson, A. M., *Physical Processes in Geology*, 577 pp., Freeman, Cooper, San Francisco, Calif., 1970.
- Melosh, J., Acoustic fluidization, *Am. Sci.*, 71, 158–165, 1983.
- Moore, H. J., G. G. Schaber, and D. W. G. Arthur, Yield strengths of flows on the Earth, Mars and Moon, *Proc. Lunar Planet. Sci. Conf.*, 9th, 3351–3378, 1978.
- Pflaker, G., and G. E. Erickson, Nevados Huascaran avalanches, Peru, in *Rockslides and Avalanches*, vol. 1, *Natural Phenomena*, edited by B. Voight, pp. 277–314, Elsevier Science, New York, 1978.
- Shreve, R. H., The Blackhawk landslide, *Spec. Pap. Geol. Soc. Am.*, 108, 47 pp., 1968.
- Stuiver, Minze, Radio-carbon time scale tested against magnetic and other dating schemes, *Nature*, 1273, 271–274, 1978.
- Tapponier, P., and P. Molnar, Slip line field theory and large scale continental tectonics, *Nature*, 264, 319–324, 1976.
- Weertman, J., The creep strength of the earth's mantle, *Rev. Geophys.*, 8, 145–168, 1970.
- Williams, H., A recent volcanic eruption near Lassen Peak, California, *Bull. Calif. Dep. Geol. Sci.*, 17, 241–263, 1928.
- D. B. Eppler, Science Applications International Corporation, 101 Convention Center Drive, Las Vegas, NV 89109.
- J. Fink, Geology Department, Arizona State University Tempe, AZ 85287.
- R. Fletcher, Center for Tectonophysics, Texas A & M University, College Station, TX 77843.

(Received May 19, 1986;  
revised December 1, 1986;  
accepted January 26, 1987.)